

GRO J0422+32: The Lowest Mass Black Hole?¹

Dawn M. Gelino

dgelino@ucsd.edu

*Center for Astrophysics and Space Sciences, Mail Code 0424, 9500 Gilman Drive,
University of California at San Diego, La Jolla, CA 92093-0424*

Thomas E. Harrison

tharriso@nmsu.edu

Department of Astronomy, New Mexico State University, Las Cruces, NM 88003

ABSTRACT

We have obtained optical and infrared photometry of the soft X-ray transient GRO J0422+32. From this photometry, we find a secondary star spectral type of M1, and an extinction of $A_V = 0.74 \pm 0.09$. We present the first observed infrared (J -, H -, and K -band) ellipsoidal variations, and model them with WD98, a recent version of the Wilson-Devinney light curve modeling code. Assuming no significant contamination of the infrared light curves, we find a lower limit to the inclination angle of 43° corresponding to an upper limit on the mass of the compact object of $4.92 M_\odot$. Combining the models with the observed spectral energy distribution of the system, the most likely value for the orbital inclination angle is $45^\circ \pm 2^\circ$. This inclination angle corresponds to a primary black hole mass of $3.97 \pm 0.95 M_\odot$. Thus we contend that J0422+32 contains the lowest mass stellar black hole reported, and the first to have a measured mass that falls in the $3 - 5 M_\odot$ range.

Subject headings: binaries: close – stars: black holes – stars: individual (J0422+32) – stars: low mass – stars: variables: other

¹This work was based on observations obtained with the Apache Point Observatory 3.5-meter telescope, which is owned and operated by the Astrophysical Research Consortium, and the 3-meter Shane telescope at Lick Observatory, which is a Multi-campus Research Unit of the University of California.

1. Introduction

Soft X-Ray Transients (SXTs) are a subset of low mass X-ray binaries that exhibit large and abrupt X-ray and optical outbursts separated by long intervals of quiescence. In most cases the compact object is a black hole and the companion star is a low-mass K- or M-type dwarf (see Charles 2001 for a review). During their periods of quiescence, SXTs are very faint at X-ray and optical wavelengths, however, in this state, the secondary stars can dominate the system luminosity and allow us to derive the parameters of the SXT binary.

J0422+32 ($\alpha_{2000} = 04^{\text{h}}21^{\text{m}}42.8^{\text{s}}$, $\delta_{2000} = 32^{\circ}54'26.6''$) was discovered by the Burst and Transient Source Experiment on the Compton Gamma Ray Observatory on 1992 August 5 (Paciesas & Briggs 1992), while the $V \sim 13$ optical counterpart was identified by Castro-Tirado et al. (1993). Since its initial outburst, J0422+32 has been studied by Filippenko, Matheson, & Ho (1995), Beekman et al. (1997), Harlaftis et al. (1999), Webb et al. (2000), and references therein. These authors have found an orbital period of 5.092 hr, a secondary star spectral type of M2±2, a mass ratio of $0.116^{+0.079}_{-0.071}$, and secondary star radial velocity semi-amplitude of $372 \pm 10 \text{ km s}^{-1}$. The implied mass function for J0422+32 is $1.13 \pm 0.09 \text{ M}_{\odot}$ (Harlaftis et al. 1999), well below that of the accepted maximum mass of a neutron star ($\sim 3.2 \text{ M}_{\odot}$).

The X-ray and optical outburst light curves of J0422+32 resemble those of the SXT prototype, V616 Mon (King, Harrison, & McNamara 1996), however, the source has exhibited recurring optical and X-ray mini-outburst behavior since 1992, reminiscent of X-ray binaries with neutron star primaries (J0422+32 is not alone in this respect, however). In order to determine the nature of the primary object in J0422+32, its mass, and therefore orbital inclination angle, must be accurately measured. As discussed in Gelino, Harrison, & McNamara (2001, hereafter Paper I) and Gelino, Harrison, & Orosz (2001, hereafter Paper II), the best way to find the inclination angle in a non-eclipsing system is to model its infrared ellipsoidal light curves. Previously, the only ellipsoidal variations detected from J0422+32 have been in the optical (Callanan et al. 1996; Chevalier & Illovaisky 1996; Casares et al. 1995; Orosz & Bailyn 1995). One previously published attempt was made to observe the variations in the infrared, where there is a smaller chance of contamination from other sources of light in the system, but even after combining the H - and K -band data, no ellipsoidal variations were seen (Beekman et al. 1997). Nonetheless, orbital inclination angle estimates have still been made. These previously published inclination angles for J0422+32 range from 10° [lower limit from Beekman et al. (1997)] to 51° [upper limit from Filippenko, Matheson, & Ho (1995)], and correspond to primary masses of 34.8 M_{\odot} and 2.4 M_{\odot} , respectively. In addition, Bonnet-Bidaud & Mouchet (1995) compared the intrinsic optical emission line widths of J0422+32 to those of V616 Mon, and found that the J0422+32 primary is a neutron star

with $M_1 \leq 2.2 M_{\odot}$.

In order to determine the mass, and therefore the nature, of the compact object in J0422+32, we have obtained J -, H -, and K -band light curves and model them here with WD98, a recent version of the Wilson-Devinney light curve modeling code. In Section 2 we describe our observations and data reduction process, as well as present the infrared photometric light curves. We describe our choices for the relevant WD98 input parameters and present our models of the variations in Section 3. Finally, in Section 4, based on the presented models, we discuss the nature of the compact object in J0422+32.

2. Observations & Data Reduction

J0422+32 was observed using GRIM II² on the Astrophysical Research Consortium 3.5 meter telescope at Apache Point Observatory on 2000 January 23, 24, 25, and 26. J -band data were obtained on all of these nights, while K_s -band data were obtained only on 2000 January 25 and 26. The data were linearized before averaging the images at one position and subtracting them from the average of the images at the other position. The images were flat fielded with a dome flat using the usual IRAF³ packages.

The SXT was observed again on 2003 February 7 and 8 using the Gemini Twin-Arrays Infrared Camera⁴ on the Shane 3 meter telescope at Lick Observatory. Simultaneous J - and K' -, and H - and K' -data were obtained. The number of counts in each exposure was kept in the linear regime of each chip, as there is no linearization correction available. These data were reduced in the same manner as above using twilight flats.

Aperture photometry was performed on J0422+32 and five nearby field stars. Using the IRAF PHOT package, a differential light curve for each band was generated separately for the 2000 and 2003 data sets, with each point being the average of four beam switched images. The differential photometric results show that over the course of our observations, the comparison stars did not vary more than expected from photon statistics. Variations were observed in both the 2000 and 2003 data sets. Figure 1 compares the 2000 and 2003 light curves.

²See <http://www.apo.nmsu.edu/Instruments/GRIM2/>

³IRAF is distributed by the National Optical Astronomy Observatories, which are operated by the Association of Universities for Research in Astronomy, Inc., under cooperative agreement with the National Science Foundation.

⁴See http://mthamilton.ucolick.org/techdocs/instruments/gemini/gemini_index.html

As Figure 1 shows, the 2000 and 2003 observations revealed light curve shapes, amplitudes, and brightnesses which were consistent with each other. This enabled us to combine both data sets. The final J , H , and K_s differential light curves of J0422+32, phased to the ephemeris of Webb et al. (2000), are presented in Figure 2. These light curves represent the first detections of infrared ellipsoidal variations from this SXT.

Optical observations of J0422+32 were obtained with SPIcam⁵ on 2001 December 18. The B -, V -, R -, and I -band exposures were bias-corrected and flat-fielded before aperture photometry was performed. Standards were also observed to transform these data to the system of Landolt. The colors of J0422+32 can be found in Table 1, along with other quiescent optical and infrared colors published for this SXT.

3. Infrared Light Curve Modeling

The J0422+32 infrared light curves presented in Figure 2 were modeled with WD98 in order to find the orbital inclination angle of the system. Many of the parameters needed for light curve modeling are based upon the nature of the secondary star. Before we can model the infrared light curves of J0422+32, we must first derive the input model parameters, and we do so here.

3.1. The Nature of the Secondary Star in J0422+32

The most important parameter for modeling the infrared light curves of any non-eclipsing system is the spectral type of the secondary star. This property can be estimated by comparing red optical spectra of the SXT secondary star with various spectral types from the same luminosity class. Because of the orbital motion of J0422+32 ($\pm 372 \text{ km s}^{-1}$), the photospheric absorption lines are broadened by rotation. This effect is usually accounted for during the analysis of the spectral data. The optical spectrum may also suffer from contamination. Both effects can weaken the apparent line strengths, and make stellar classification difficult. Another difficulty is that to classify the secondary star in these systems, it is assumed that the gravity and abundances of the secondary star are consistent with those of the main sequence templates used to derive the spectral type. Given the low S/N of these data, deriving a spectral type can be challenging.

Alternatively, one can use a spectral energy distribution (SED), and the above limits

⁵See <http://www.apo.nmsu.edu/Instruments/SPIcam/>

on the spectral type to not only derive an effective temperature of the secondary star, but also estimates for both the visual extinction and contamination level. Although difficulties similar to finding the spectral type of the secondary star from spectra may be encountered when using broad-band photometry, the effective temperature is less sensitive to changes in the gravity and abundances than the shape and depth of individual spectral features. Given the higher S/N an effective temperature derived using photometry can be just as useful as a spectral type derived from the spectroscopic data set. We present the optical-infrared (*BVRJHK*) SED for J0422+32 in Figure 3. In this figure we compare the observed SED to those for an M1V and an M4V (Bessell & Brett 1988; Bessell 1991; Mikami & Heck 1982). We find that after dereddening the observed data by $A_V=0.74$ mags, the best-fitting spectral type is that of an M1V. This extinction is consistent with published values. Shrader et al. (1994) calculate $E(B-V)=0.2\pm0.1$ from the 5780Å diffuse interstellar feature, $E(B-V)=0.23\pm0.02$ from an optical continuum power law fit, and finally $E(B-V)=0.40\pm0.06$ from an ultraviolet 2170Å interstellar feature. Our color excess of $E(B-V)=0.24\pm0.03$ from SED fitting is consistent with the optically derived excess from Shrader et al. (1994), as well as those from King, Harrison, & McNamara (1996), Callanan et al. (1995), and Martin et al. (1995). Based on the results from Figure 3, we adopt an extinction value of $A_V=0.74\pm0.09$ mag, a secondary star spectral type of M1, and corresponding temperature of $T_{\text{eff}} = 3900$ K (Gray 1992).

An M1V spectral type is consistent with those found by Casares et al. (1995) and Harlaftis et al. (1999), but not with the M4V type arrived at by Webb et al. (2000). A spectral type of M4V cannot be made consistent with the observations, no matter the extinction. The only way to make a spectral type as late as M4 work with the observations is to posit the existence of an additional source of blue luminosity in the system. However, as is clear from the SED, such a source would have to supply 70% of the flux in the *R*-band, and would dominate the red optical spectra. We address the issue of contamination in the next section.

It can be seen from Table 1 that the infrared data presented by Beekman et al. (1997) are not consistent with our photometry. While the optical magnitudes and colors have shown very little evidence for change since J0422+32 entered quiescence, the infrared luminosity of the source appears to have declined by more than a magnitude! By combining data from Casares et al. (1995) with that of Beekman et al. (1997) taken within the same month, we find that $V - K = 6.12$ in 1994. If we assume that $A_V=0.74$, the dereddened value is $(V - K)_0 = 5.46$. This corresponds to a spectral type of M4/5V. Using the dereddened color from Casares et al. (1995), $(V - I)_0 = 1.72$, a spectral type of $M0V \pm 1$ is derived. These two colors are completely inconsistent: the $V - I$ color of an M4/5V would be 3.0 ± 0.2 ! This should be compared with our values of $(V - I)_0 = 1.96$ (M1V), and $(V - K)_0 = 3.95$ (M1V).

It seems difficult to understand this type of change. We have examined the 2MASS values for the secondary standards used by Beekman et al. (1997), and have been unable to reproduce their photometry. First, in the notes of their Table 2, they appear to have confused the identification of their two standard stars with those of Chevalier & Ilovaisky (1995). Chevalier & Ilovaisky (1995) star #4 is the brighter of the two stars, and must correspond to their “Standard-1” (although it is possible that star #4 is variable, no evidence to this effect is found in our long-term data). Even with the correct identification, however, their photometry does not agree with the 2MASS values. If there was simply a zero point offset, the differences between the two sets of magnitudes would be consistent. We do not find any such consistency. We are unable to determine the source of this problem, but there does appear to be something unusual about the Beekman et al. (1997) infrared photometry that extends beyond a mere zero point correction.

We conclude that the spectral type of the secondary star is M1V+/-1, consistent with all of the previous assignments, except that of Webb et al. (2000). While the methodology used by Webb et al. (2000) is robust for normal, late-type main sequence stars, it is unclear whether the secondary stars in SXTs can be considered to be normal main sequence stars. Again, broad-band photometry is not as sensitive to changes in gravity and abundances as spectral features, however we do use main sequence data in the SED and atmosphere models (see section 3.3). Therefore, for completeness, we have run models where the spectral type of the secondary star was assigned an effective temperature of an M4V, the spectral type determined by Webb et al. (2000). We find that our result does not significantly change with this variation in spectral type.

3.2. Estimating the Amount of Infrared Non-Stellar Light

If we assume a spectral type of M1V and $A_V=0.74$ mags, there is very little room in the $VRIJHK$ SED for contamination from other sources in the system. Because the level of contamination is an extremely important quantity, acting to dilute the ellipsoidal variations, we address the issue here. There have been a number of estimates for the level of the R -band contamination in the J0422+32 system ranging from less than 20% (Callanan et al. 1996) to up to 60% (Casares et al. 1995; Filippenko, Matheson, & Ho 1995). In our SED, we find that there is about an 8% *excess* in the R -band that could be attributed to $H\alpha$ emission. Estimating the level of contamination in an optical spectrum that has limited wavelength coverage is more difficult than spectral type determination—it suffers from many of the same issues, while attempting to fit a continuum to the observed spectrum.

It is clear from the SED that combinations of a hot and a cool source can reproduce the

observed spectrum. But note that whatever “hot” source (anything hotter than an M1V) one selects so as to reproduce the *BVRI* data by combining it with a very late-type dwarf, it will have only minor effects in the infrared. No one has proposed a spectral type later than M4 for the secondary star. If one chooses an M4V spectral type for the companion, and normalize the SED to the observed *K*-band flux, then the secondary star only supplies 30% of the observed *R*-band flux. This fraction, of course, is even smaller if you don’t normalize to the *K*-band flux. Thus, the level of contamination in the *R*-band using an M4 secondary star, 70%, is larger than any of the existing estimates for this contamination. The optical spectrum of such a heavily contaminated source would be highly diluted, and quite difficult to extract. As one adjusts the spectral type of the companion to earlier types, the dilution is lessened. An M2V would have a dilution of 24% at *R*, with the star contributing 76% of the flux.

The most difficult contamination source to extract in the case of J0422+32 is the one that has the *shallowest spectral slope*. The most relevant emission process with the shallowest slope is free-free emission, which in λF_λ space has a spectrum proportional to λ^{-1} . If we ascribe the entire B-band excess (34%) to free-free emission, then in the *K*-band, the contamination would be $\sim 7\%$. Such a low-level of contamination would be difficult to detect given the S/N of the current data. *Any other proposed process, such as synchrotron emission, or classical accretion disk spectra produces a steeper spectrum in λF_λ than free-free emission, and thus will dilute the infrared ellipsoidal variations by a smaller amount than free-free emission.*

A very conservative estimate of the disk contamination in the infrared is based on the assumption that the optically thin disk indeed radiates through free-free emission processes. A 7% contamination in the infrared bands would cause the observed orbital inclination angle of the system to be underestimated by $\leq 2^\circ$.

3.3. Ellipsoidal Models

As in Papers I and II, we modeled the infrared light curves of J0422+32 with WD98 (Wilson 1998). See Paper I for references and a basic description of the code, and Gelino (2001) for a more comprehensive description. We ran WD98 for a semi-detached binary with the primary having such a large gravitational potential, that it essentially has zero radius. The most important adopted wavelength-independent input values to WD98 are listed in Table 2, and the wavelength-dependent values are listed in Table 3.

The models were run for a range of inclination angles with parameters for an M0V through an M4V secondary star. The secondary star atmosphere was determined from solar-

metallicity Kurucz models. The Kurucz atmosphere models are computed in temperature steps of 250 K for the range we are interested in, and stop at 3500 K. We therefore use extrapolated fluxes for the cooler parts of the star. For reasons cited above, we have used normal, non-irradiated, limb darkening coefficients in the models (van Hamme 1993). We also adopted gravity darkening exponents found by Claret (2000), and a mass ratio, q , of $0.116^{+0.079}_{-0.071}$ (Harlaftis et al. 1999). We ran models assuming the secondary star was the only source of *infrared* light in the system. We also assumed that the secondary star had a uniform surface brightness aside from limb- and gravity-darkening effects (i.e. no star spots).

The best fit model was determined using χ^2 tests. We found that changing the spectral type of the secondary from an M4V to an M0V, resulted in a change in the orbital inclination angle of $<1^\circ$. Similarly, varying q from 0.045 to 0.195 affected i by $\leq 1^\circ$. We find that the best fitting J -, H -, and K_s -band model has $i = 45^\circ$, and the parameters found in Table 2. Figure 2 presents this best fitting model for the J -, H -, and K_s -band light curves.

3.4. The Adopted Model and its Uncertainties

Assuming all of the infrared light in the system comes from the secondary star, the best fitting orbital inclination angle for J0422+32 is $i = 45^\circ$. If this assumption was incorrect, and significant infrared contamination were present in the system, each light curve would most likely be diluted by a different amount, causing the best fit inclination for each band to be different from the others. We instead find that all three infrared light curves give a consistent 45° best fit whether solved simultaneously or individually.

If there is no contamination affecting the infrared light curves, the absolute lower limit to the inclination angle is 43° . This corresponds to an upper limit to the compact object mass of $4.92 M_\odot$, firmly placing it below $5 M_\odot$. Using an estimate of 7% for the infrared accretion disk contamination in the system gives an inclination of $45^{+2.80}_{-2}$, however, we do not believe that the infrared light curves are significantly affected by any such contamination. Therefore, based on the error in q , the spectral type (i.e. temperature) of the secondary star, and the photometric error bars, the adopted orbital inclination angle is $45^\circ \pm 2^\circ$. Combining this inclination with the observed mass function, we find the mass of the primary object to be $3.97 \pm 0.95 M_\odot$.

Using the mass of the compact object and the orbital period, the orbital separation of the two components in the system can be computed. This in turn, can be combined with the mass ratio to find the size of the Roche lobe for the secondary star. The temperature of the secondary and its Roche lobe radius are then used to find the secondary's bolometric lumi-

nosity and bolometric absolute magnitude. After accounting for the bolometric correction (Bessell 1991), the distance modulus for the J , H , and K bands is used to find an average distance of 2.49 ± 0.30 kpc. Table 4 lists all of the derived parameters for J0422+32.

4. Discussion

In this paper, we have presented the first observed infrared ellipsoidal variations for J0422+32. The derived parameters in Table 4 are based on the modeling of these variations assuming no significant contamination from any other sources of infrared light in the system. Even though there is a large range of published inclination angles for this system, the inclination angle found here is consistent with those found by Orosz & Bailyn (1995, $\geq 45^\circ$), Filippenko, Matheson, & Ho (1995, 45° – 51°), Callanan et al. (1996, $< 45^\circ$), and Webb et al. (2000, $\leq 45^\circ$), and suggests that we should not be overly surprised that this system harbors a low-mass object.

Even though the errors determined here for the orbital inclination angle and mass of the primary object are smaller than previously published, the nature of the primary object in this system remains unclear. Both the optical and X-ray outburst light curves of J0422+32 closely resemble those of the prototype black hole SXT, V616 Mon. However, since outburst, the system has exhibited a series of mini-outbursts, similar to those observed from neutron star X-ray binaries such as Aql X-1 (Charles et al. 1980). Martin et al. (1995) not only compare this SXT with Aql X-1, but also compare J0422+32 to GX 339-4, an X-ray binary system thought to be a black hole candidate based on its rapid X-ray variability, and because it exhibits “high,” “low,” and “off” states (Markert et al. 1973). They conclude their study by saying, “J0422+32 would seem to be a system whose nature is intermediate between the X-ray transients and those which show more than one mode of accretion.”

We find the minimum mass of the primary object to be just below the maximum accepted mass for a neutron star. However, just about all neutron stars with measured masses cluster around $1.35 M_\odot$ with a small spread of $\pm 0.04 M_\odot$ (van Kerwijk 2001). For the compact object in this system to have a mass consistent with that of a typical neutron star, the orbital inclination angle would have to be about 85° , which is ruled out by a lack of eclipses during outburst. In addition, contamination at the 160% level in the infrared is needed to account for a 40° underestimation of the inclination angle. This level of contamination surely would be visible in the SED, and rule out any possibility of detecting the secondary star in the optical, therefore until more compelling evidence for a neutron star primary is presented, we suggest that the primary object in J0422+32 is a low mass black hole.

Recently, two papers (Paper II; Greiner, Cuby, & McCaughrean (2001)) have published evidence for the highest-mass stellar black holes. Here we find what appears to be the lowest mass stellar black hole. A handful of other sources may be potential candidates based on their observed mass functions, but current findings suggest otherwise. The most likely candidate to join J0422+32 as a low mass black hole is GRS 1009-45. The current estimates of the compact object mass span from $4.64M_{\odot}$ to $5.84 M_{\odot}$ (Gelino 2002) with a lower limit of $4.4M_{\odot}$ from lack of X-ray eclipses (Filippenko et al. 1999). Thus we contend that J0422+32 contains the lowest mass stellar black hole, and the first to have a measured mass that falls in the $3 - 5 M_{\odot}$ range.

We would like to thank John Tomsick for helpful discussions, and the Apache Point Observatory and Lick Observatory staff, especially Elinor Gates. DMG held an American Fellowship from the American Association of University Women Educational Foundation while working on this project in 2000, and currently holds a CASS Postdoctoral Fellowship.

REFERENCES

Beekman G., Shahbaz, T., Naylor, T., Charles, P. A., Wagner, R., & Martini, P. 1997, MNRAS, 290, 303

Bessel, M. S. 1991, AJ, 101, 662

Bessell, M. S. & Brett, J. M. 1988, PASP, 100 1134

Bonnet-Bidaud, J. & Mouchet, M. 1995, A&A, 293, L69

Callanan, P. J., et al. 1995, ApJ, 441, 786

Callanan, P. J., Garcia, M., Filippenko, A. V., McLean, I., & Teplitz, H. 1996, ApJ, 470, L57

Casares, J., Martin, A., Charles, P. A., Martín, E., Rebolo, R., Harlaftis, E., & Castro-Tirado, A. 1995, MNRAS, 276, L35

Castro-Tirado, A. J., Pavlenko, E. P., Shlyapnikov, A. A., Brandt, S., Lund, N., & Ortiz, J. L. 1993, A&A, 276, L37

Charles, P. A. et al. 1980, ApJ, 237, 154

Charles, P. A. 2001, in Black Holes in Binaries and Galactic Nuclei, eds. L. Kaper, E. P. J. van den Heuvel, & P. A. Woudt, (Berlin: Springer), 27

Chevalier, C. & Ilovaisky, S. 1995, A&A, 297, 103

Chevalier, C. & Ilovaisky, S. 1996, A&A, 312, 105

Claret, A. 2000, A&A, 359, 289

Filippenko, A. V., Leonard, D. C., Matheson, T., Li, W., Moran, E. C., & Riess, A. G. 1999, PASP, 111, 969

Filippenko, A. V., Matheson, T., & Ho, L. 1995, ApJ, 455, 614

Garcia, M. R., Callanan, P. J., McClintock, J. E., & Zhao, P. 1996, ApJ, 460, 932

Gelino, D. M. 2001, PhD Thesis, New Mexico State University

Gelino, D. M. 2002, BAAS, 34, 654

Gelino, D. M., Harrison, T. E., & McNamara, B. J. 2001, AJ, 122, 971 (Paper I)

Gelino, D. M., Harrison, T. E., & Orosz, J. A. 2001, AJ, 122, 2668 (Paper II)

Gray, D. F. 1992, Cambridge Astrophysics Series #20, The Observations and Analysis of Stellar Photospheres (New York: Cambridge University Press)

Greiner, J., Cuby, J. G., & McCaughrean, M. J. 2001, Nature, 414, 522

Harlaftis, E. T., Collier, S., Horne, K., & Filippenko, A. V. 1999, A&A, 341, 491

King, N. L., Harrison, T. E., & McNamara, B. J. 1996, AJ, 111, 1675

Markert, T. H., Canizares, C. R., Clark, G. W., Lewin, W. H. G., Schnopper, H., W., & Sprott, G. F. 1973, ApJ, 184, L67

Martin, A. C., Charles, P. A., Wagner, R. M., Casares, J., Henden, A. A., & Pavlenko, E. P. 1995, MNRAS, 274, 559

Mikami, T. & Heck, A. 1982, PASJ, 34, 529

Orosz, J. A. & Bailyn, C. D. 1995, ApJ, 446, L59

Paciesas W. S., & Briggs M. S. 1992, IAU Circ. 5580

Shrader, C. R., Wagner, R. M., Hjellming, R. M., Han, X. H., & Starrfield, S. G. 1994, ApJ, 434, 698

van Hamme, W. 1993, AJ, 106, 2096

van Kerkwijk, M. H. 2001, in Black Holes in Binaries and Galactic Nuclei, eds. L. Kaper, E. P. J. van den Heuvel, & P. A. Woudt, (Berlin: Springer), 39

Webb, N. A., Naylor, T., Ioannou, Z., Charles, P. A., & Shahbaz, T. 2000, MNRAS, 317, 528

Wilson, R.E. 1998, in Reference Manual to the Wilson-Devinney Program, Computing Binary Star Observables, Version 1998 (Gainesville, FL: Univ. Florida)

Zhao, P., Callanan, P., Garcia, M., & McClintock, J. 1994, IAU Circ. 6072

Table 1. Quiescent Infrared and Optical Colors of J0422+32

Reference	V	V - R	V - I	K	J - K	H - K	Date ^a
1	22.39±0.27	1.33±0.29	9/93
2	22.24±0.14	1.27±0.17	2.02±0.16	12/94
3	16.12±0.04 ^b	...	0.31±0.05 ^b	12/94
4	22.3±0.2	1.3±0.2	9/94–1/95
5	22.35±0.17	1.41±0.20	9/94–3/95
6	22.05±0.10 ^c	1.31±0.12	2.26±0.12	17.44±0.09	0.95±0.10	0.16±0.16	2000/2001/2003

^aMonth and year the data were obtained

^bData cannot be reconciled with 2MASS, see text

^cB-V=1.17±0.17

References. — (1) Zhao et al. (1994) (2) Casares et al. (1995) (3) Beekman et al. (1997) (4) Callanan et al. (1996) (5) Garcia et al. (1996) (6) This Paper

Table 2. Wavelength-Independent WD98 Input Parameters

Parameter	Value
Orbital Period (days)	0.2121600
Ephemeris (HJD phase 0.0) ^a	2450274.4156
Orbital Eccentricity	0.0
Temperature of Secondary (K)	3900
Mass Ratio (M_2/M_1)	0.116
Atmosphere Model	Kurucz ($\log g = 4.59$)
Limb Darkening Law	Square-root
Secondary Star Gravity Darkening Exponent	$\beta_1=0.27$
Secondary Star Bolometric Albedo	0.676

^aFrom Webb et al. (2000)

Table 3. Wavelength-Dependent WD98 Input Parameters

Parameter	J	H	K
Square-root Limb Darkening Coefficient x_λ	-0.137	-0.146	-0.160
Square-root Limb Darkening Coefficient y_λ	0.718	0.655	0.592

Table 4. Derived Parameters for J0422+32

Parameter	Value
Orbital Inclination Angle ($^\circ$)	45 \pm 2
Primary Object Mass M_1 (M_\odot)	3.97 \pm 0.95
Secondary Star Mass M_2 (M_\odot)	0.46 \pm 0.31
Orbital Separation a (R_\odot)	2.45 \pm 0.24
Secondary Star Radius R_{L_2} (R_\odot)	0.53 \pm 0.16
Adopted Distance (kpc)	2.49 \pm 0.30

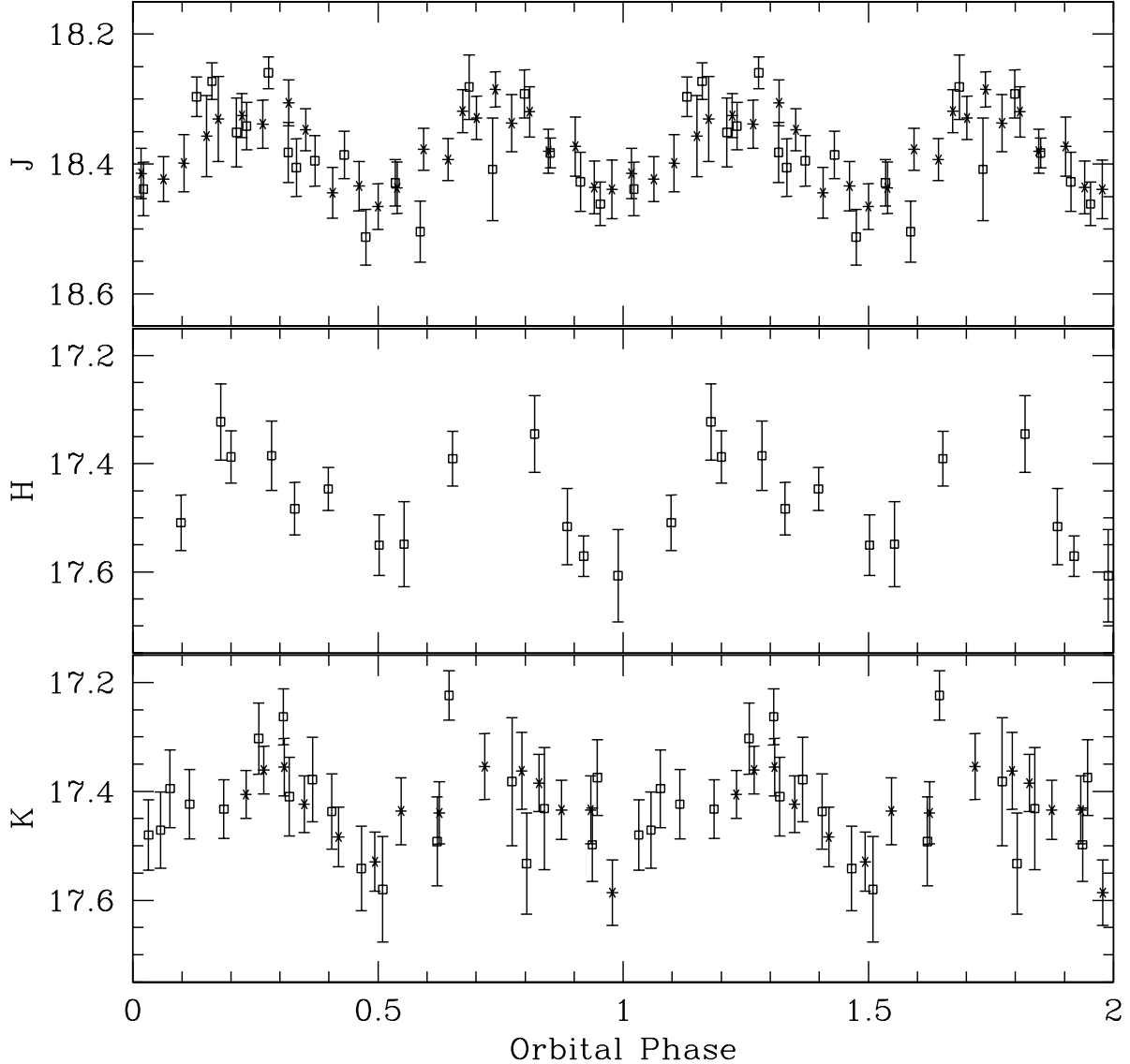


Fig. 1.— Top panel: Long-term infrared light curves of J0422+32. The J - and K -band data span 37 months. The asterisks represent data taken January 2000 with the Astrophysical Research Consortium 3.5 m telescope, and the open squares represent data taken February 2003 with the Lick Observatory Shane 3 m telescope. Error bars are $1-\sigma$. These data are plotted over two phase cycles for clarity. Here, and throughout this paper, we phase the J0422+32 heliocentric-corrected data to the ephemeris of Webb et al. (2000). There are no obvious long-term variations in the shapes or mean magnitudes of the light curves.

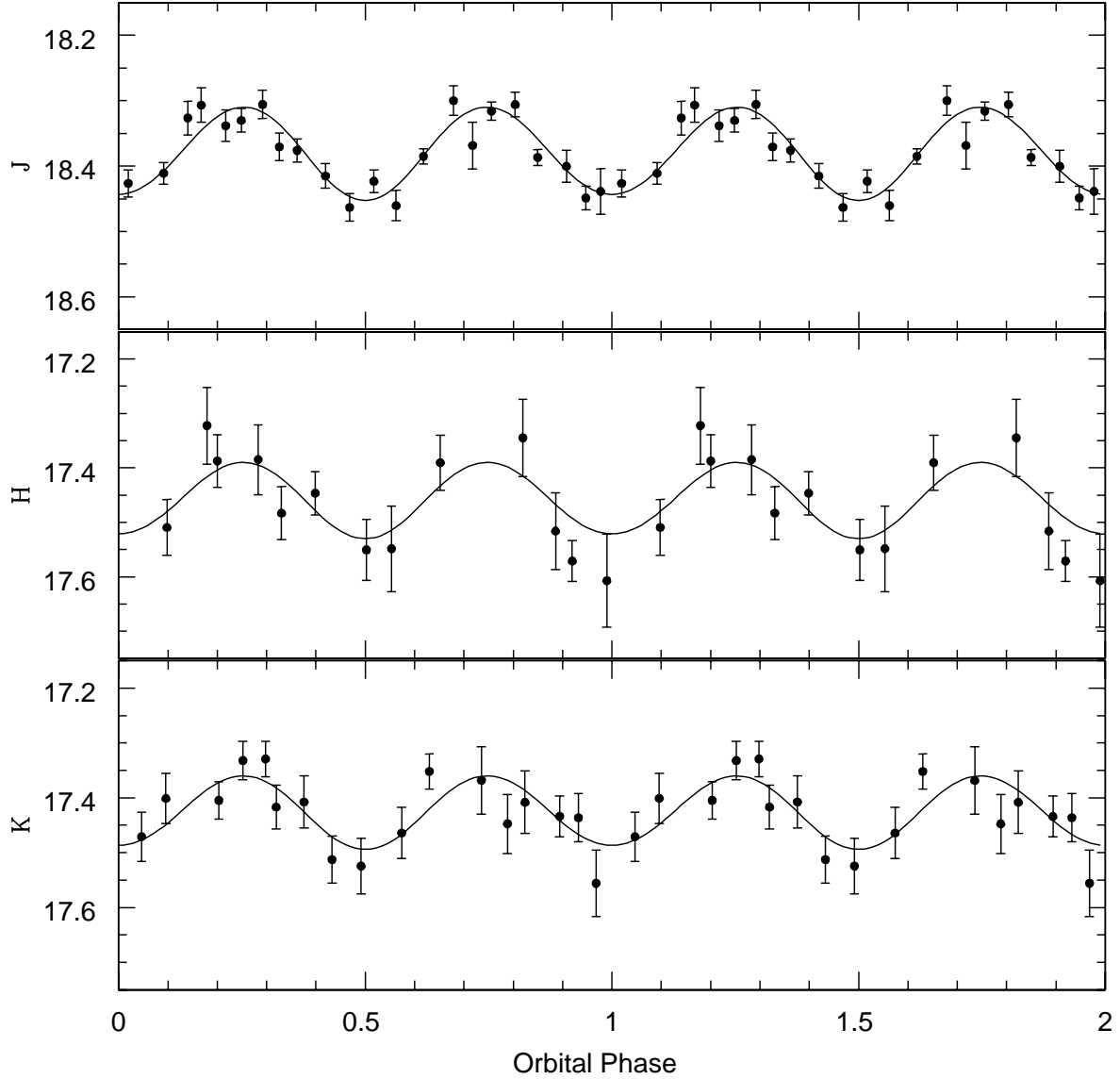


Fig. 2.— J0422+32 J -, H -, and K -band final light curves (points). Error bars are $1-\sigma$. The solid line represents the best fitting ($i = 45^\circ$) WD98 model as described in the text.

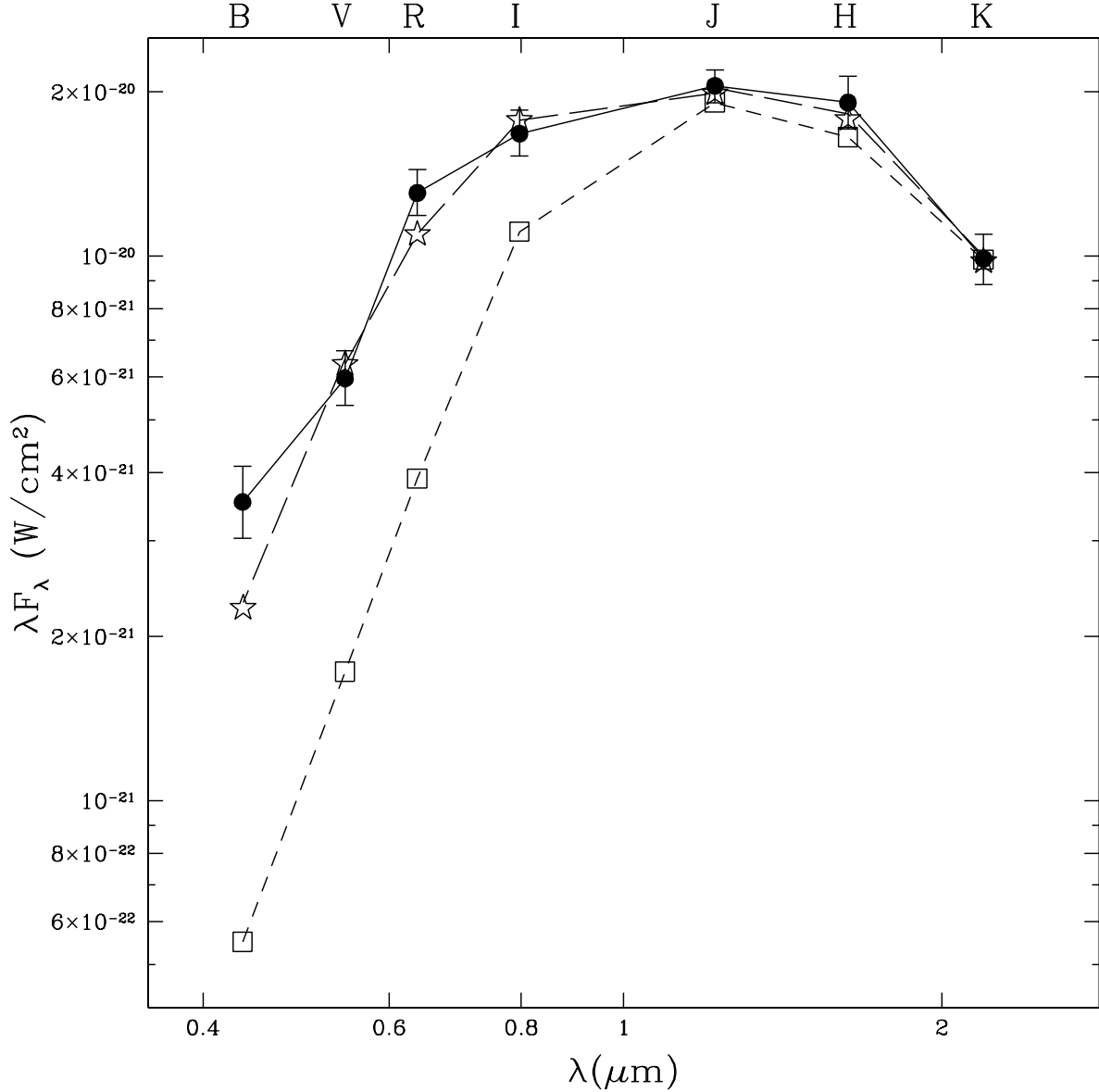


Fig. 3.— J0422+32 optical/infrared quiescent SED dereddened by $A_V = 0.74$ mag (filled circles). The infrared (JHK) points represent phase-averaged data. Error bars are 1σ . These data are compared to the SED for an M1V (open stars), and an M4V (open squares), normalized at K . The M1V SED fits that of J0422+32 with exceptions at B (34%) and R (8%).